



0010-938X(94)00109-X

## A COMPARATIVE STUDY ON THE PASSIVATION AND LOCALIZED CORROSION OF $\alpha$ - AND $\beta$ -BRASS IN BORATE BUFFER SOLUTIONS CONTAINING SODIUM CHLORIDE—II. X-RAY PHOTOELECTRON AND AUGER ELECTRON SPECTROSCOPY DATA

J. MORALES,\* P. ESPARZA,\* G. T. FERNANDEZ,\* S. GONZALEZ,\*  
J. E. GARCIA,† J. CACERES,† R. C. SALVAREZZA‡  
and A. J. ARVIA‡

\*Dpto. de Química Física, Universidad de La Laguna, Tenerife, Spain

†Dpto. de Edafología, Universidad de La Laguna, La Laguna, Tenerife, Spain

‡INIFTA, Sucursal 4, Casilla de Correo 16, (1900) La Plata, Argentina

**Abstract**—The composition of corrosion layers formed on  $\alpha$ -,  $\beta$ - and ( $\alpha + \beta$ )-brass anodized in the passive region in borate–boric acid buffer and 0.5 M NaCl + borate–boric acid buffer (pH 9) was studied comparatively by X-ray photo-electron and Auger electron spectroscopy. Passivation of brass in both solutions involves the formation of a complex passive layer consisting of ZnO and Cu<sub>2</sub>O. In both solutions, the ZnO electroformation results in a dezincification so that a thin Cu rich layer is formed at the alloy/metal oxide interface. Passive layer composition and dezincification of the alloy surface explain the localized corrosion resistance of brass as compared to polycrystalline Cu and Zn.

### INTRODUCTION

The electrochemistry of brass is particularly interesting because it offers the possibility of investigating the influence of several aspects inherent to alloy composition and structure on their corrosion and passivation behaviour in different aqueous environments. In the case of brass, corrosion, passivation and localized corrosion resistance in different aqueous solutions can be compared to the behaviour of polycrystalline Cu and Zn.

In part I, the passivity and localized corrosion resistance of  $\alpha$ -,  $\beta$ - and ( $\alpha + \beta$ )-brass in boric acid–sodium borate buffer (pH 9) +  $x$  M NaCl ( $0.01 \leq x \leq 0.5$ ), at 25°C, have been studied by using electrochemical techniques.<sup>1</sup> The electrochemical behaviour of these alloys has been interpreted in terms of their own passive layer film and dezincified alloy surface. It was observed that pitting corrosion of brass takes place at potentials slightly more negative than those of Cu and markedly more positive than that of Zn. The lower resistance of brasses as compared to Cu was assigned to the presence of a complex ZnO ·  $x$ H<sub>2</sub>O/Cu<sub>2</sub>O–CuO layer which is less protective towards Cl<sup>-</sup>-ion attack than the Cu<sub>2</sub>O–CuO layer.<sup>1</sup> Accordingly, the pitting resistance of brasses increases from ( $\alpha + \beta$ )- and  $\beta$ -brass to  $\alpha$ -brass, the latter approaching the behaviour of Cu. The increase in the pitting corrosion resistance of brass as compared to Zn was assigned to the formation of a Cu rich layer at the alloy

surface due to the electrodisolution of Zn to form  $Zn^{2+}$  and  $ZnO \cdot xH_2O$  leading to alloy dezincification. The Cu rich layer turns the alloy immune to corrosion at negative potentials.

This paper deals with a X-ray photo-electron (XPS) and Auger electron (AES) spectroscopic study on the resulting passive layer and first layers of brass after passivation in borate–boric and 0.5 M NaCl + borate–boric acid buffer at 25°C. Results confirm the passive layer composition already proposed from electrochemical data analysis.<sup>1</sup> The presence of a Cu rich surface layer at the alloys which confers their higher localized resistance in relation to Zn in NaCl-containing solutions has been conclusively proven.

## EXPERIMENTAL METHOD

Working electrodes (specimens) were made from  $\alpha$ - and  $\beta$ -brass rods with the following chemical composition (wt%):  $\alpha$ -brass, 71.719 Cu, 28.228 Zn, 0.011 C, 0.008 Al, 0.031 Sn, 0.001 As;  $\beta$ -brass, 52.460 Cu, 47.490 Zn, 0.026 C, 0.005 Al, 0.023 Sn, As and Si < 0.001.

A detailed description of the electrode preparation and electrochemical set up is given in Ref. 1. Potentials in the text are given on the saturated calomel reference electrode (SCE) scale.

XPS and AES surface analysis of  $\alpha$ - and  $\beta$ -brass specimens after anodization at 0 V in borate–boric acid buffer (0.075 M  $Na_2B_4O_7$  + 0.15 M  $H_3BO_3$ , pH 9) and in the same buffer solution containing 0.5 M NaCl at 25°C were performed. In both solutions, the anodization potential was set in the passivity range of brass.<sup>1</sup> The following experimental procedure was employed. First, specimens were electroreduced at  $-1.4$  V for 2 min to avoid any interference due to air formed films. Subsequently, the applied potential was held at 0 V for 1 min for passive layer growth. Then, specimens were removed from the cell, rinsed several times with de-aerated distilled water, dried under nitrogen and mounted in the XPS vacuum chamber. The above mentioned passivation conditions were chosen on the basis of previous work<sup>2</sup> in which it was found that the passive layer growth on Cu in borate–boric acid buffer (0.075 M  $Na_2B_4O_7$  + 0.15 M  $H_3BO_3$ , pH 9) and in the same buffer solution containing 0.5 M NaCl at 25°C was almost completed in less than 1 min. In future work it would be interesting to look at the composition of the surface layers after longer passivation times.

XPS and AES spectra were made in a Kratos XSAM instrument at a pressure of  $2 \times 10^{-9}$  Pa, using Al  $K\alpha$  radiation (1486.6 eV) for photo-electron lines in the fixed analyser transmission (FAT) detector mode, and Mg  $K\alpha$  radiation (1253.6 eV) for Auger lines in the fixed retarding ratio (FRR) detector mode. Energy levels in all samples were calibrated using the  $C_{1s}$  line. Spectral line identification was based on data provided in Ref. 3. Auger lines were analysed by deconvoluting (Lorentzian algorithm) the background substrated and smoothed spectra. The area of each contribution to a given spectral band was obtained applying the same method. Depth profiles of samples were obtained by surface sputtering with a Kratos Ion Gun at a  $0.15 \pm 0.02$  nm min<sup>-1</sup> rate. Values of  $E_b$ , the binding energy, and  $E_k$ , the kinetic energy, of standard samples are assembled in Table 1.

Table 1. Binding energy ( $E_b$ ) and kinetic energy ( $E_k$ ) of the standard samples

Sample	Energy level	$E_b$	$E_k$
Cu	2p <sub>3/2</sub>	932.3	
	LMM	334.6	919.0
Cu <sub>2</sub> O	2p <sub>3/2</sub>	932.5	
	LMM	336.6	917.0
CuO	2p <sub>3/2</sub>	933.6	
	LMM	336.0	917.6
Zn	2p <sub>3/2</sub>	1021.5	
	LMM	261.4	992.2
ZnO	2p <sub>3/2</sub>	1021.7	
	LMM	265.2	988.4

## EXPERIMENTAL RESULTS

The Zn/Cu atomic ratio from the  $2p_{3/2}$  XPS lines vs the sputtering time ( $t_s$ ) plots for those specimens passivated at 0 V in the borate–boric acid and in the borate–boric acid + 0.5 M NaCl are shown in Fig. 1. From the time required to reach a constant Zn/Cu atomic ratio close to that expected for bulk alloy it can be concluded that the passive and alloy corrosion layer thicknesses are  $d \cong 5$  nm and  $d \cong 15$  nm in borate–boric acid and in borate–boric acid + 0.5 M NaCl, respectively. These results also indicate the presence of an outer Zn-rich corrosion layer. However, a clearcut distinction between metal and its oxide in the passive and alloy corrosion layer by XPS is not feasible because of the small difference in the chemical shifts of Cu and Zn 2p photo-electrons but they can be easily identified by AES lines, namely, the  $L_3M_{45}M_{45}$  transition for Cu,  $Cu_2O$ , Zn and ZnO. Hence, AES lines were used to study the composition of the passive and the first alloy surface layers.

AES spectra of  $\alpha$ - and  $\beta$ -brass after passivation at 0 V borate–boric acid buffer are shown in Fig. 2a. As already reported for oxidized brass at low temperature ( $T < 373$  K),<sup>4</sup> the passive layer formed after anodization in this buffer consists mainly of ZnO and  $Cu_2O$ . Similar results are obtained for  $\alpha$ - and  $\beta$ -brass after passivation at 0 V in the borate–boric acid buffer containing 0.5 M NaCl (Fig. 2b).

The  $Cu_2O/Cu$  and ZnO/Zn AES line intensity ratio vs  $t_s$  plots for passivated brass specimens provide further information about the surface composition and depth profile of surface layers.

In the absence of NaCl (Fig. 3a) the  $Cu_2O/Cu$  Auger line intensity ratio in passivated  $\alpha$ -brass is very low and decreases with  $t_s$ , whereas the ZnO/Zn Auger line intensity ratio decreases sharply for  $t_s < 30$  min and smoothly afterwards. For anodized  $\beta$ -brass (Fig. 3b) the  $Cu_2O/Cu$  ratio increases with  $t_s$ , whereas the behaviour of the ZnO/Zn ratio is qualitatively comparable to that of  $\alpha$ -brass. Thus,

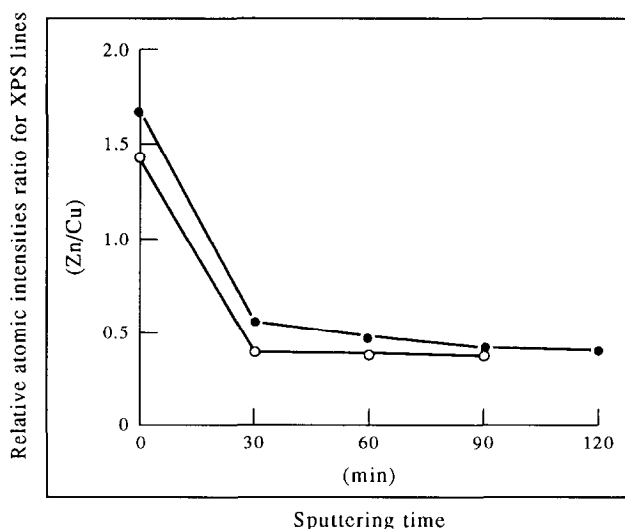


Fig. 1. Zn/Cu XPS  $2p_{3/2}$  line intensity ratio vs sputtering time plots for the  $\alpha$ -brass electrodes passivated at 0.0 V during 1 min in borate–boric acid buffer (○); and borate–boric acid buffer + 0.5 M NaCl (●).

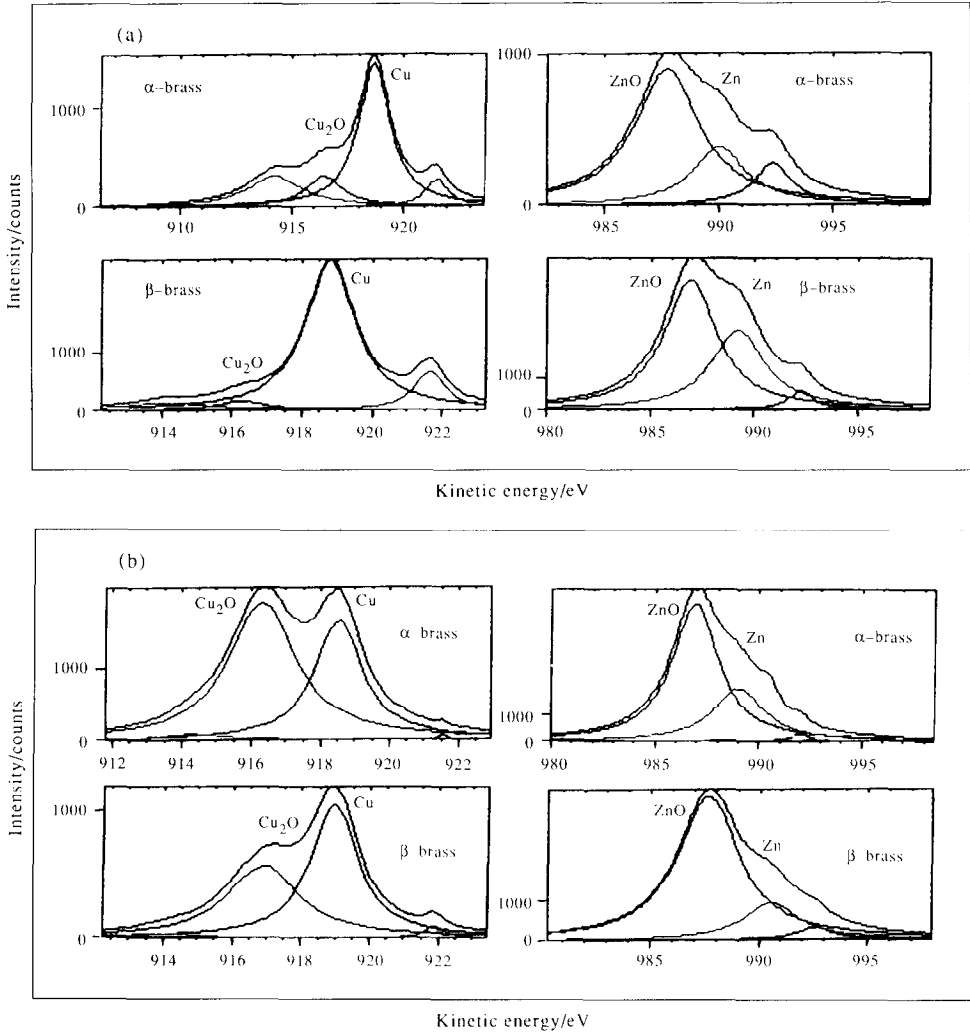


Fig. 2. Auger spectra for  $\alpha$  and  $\beta$  brass after passivation in (a) borate-boric acid buffer; and (b) borate-boric acid buffer + 0.5 M NaCl.

as observed for oxidized  $\alpha$ - and  $\beta$ -brass at  $T < 373$  K,<sup>4</sup> the outer region of the passive layer formed on  $\alpha$ -brass is richer in  $\text{Cu}_2\text{O}$  than that formed on  $\beta$ -brass. This is clearly seen from the evolution in depth of the ZnO/ $\text{Cu}_2\text{O}$  ratio for both alloys (Fig. 3c). Values of  $h$ , the passive layer thickness, formed for both alloys are roughly the same,  $h \cong 4$  nm.

The ZnO/Zn and the  $\text{Cu}_2\text{O}/\text{Cu}$  AES line intensity ratios for  $\alpha$ -brass specimens passivated in 0.5 M NaCl-containing borate-buffer (Fig. 4a) change in depth in a similar way to that observed in the absence of NaCl. Both ratios decrease with  $t_s$  to attain nearly constant values. However, in the NaCl containing buffer  $h \cong 15$  nm, a figure greater than that found in plain buffer. The oxide/metal ratio vs  $t_s$  plot for passivated  $\beta$ -brass specimens in the 0.5 M NaCl containing buffer (Fig. 4b) is qualitatively comparable to that observed for passivated  $\alpha$ -brass. It should be noted that for this

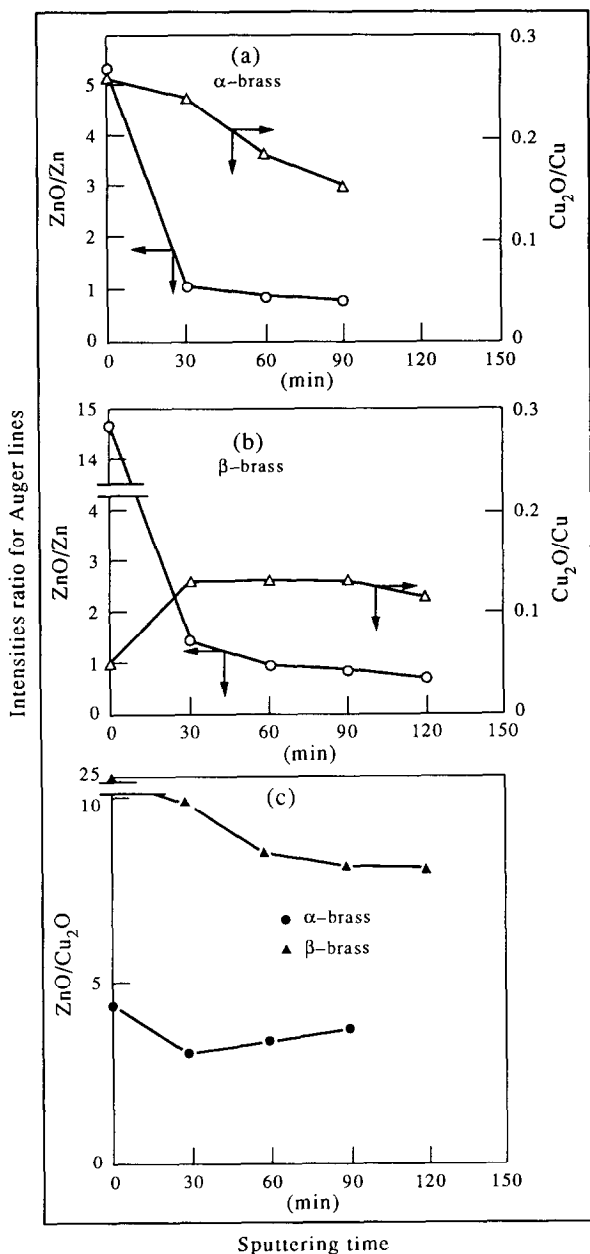


Fig. 3. Metal/oxide  $L_{3}M_{45}M_{45}$  Auger line intensity ratio vs sputtering time plots. (a)  $\alpha$ -brass passivated at 0.0 V in borate-boric acid buffer, ( $\Delta$ ) Cu<sub>2</sub>O/Cu, ( $\circ$ ) ZnO/Zn; (b)  $\beta$ -brass passivated at 0.0 V in borate-boric acid buffer, ( $\Delta$ ) Cu<sub>2</sub>O/Cu, ( $\circ$ ) ZnO/Zn; and (c) ZnO/Cu<sub>2</sub>O  $L_{3}M_{45}M_{45}$  Auger line intensity ratio vs sputtering time for ( $\bullet$ )  $\alpha$ -brass and ( $\blacktriangle$ )  $\beta$ -brass passivated at 0.0 V in borate-boric acid.

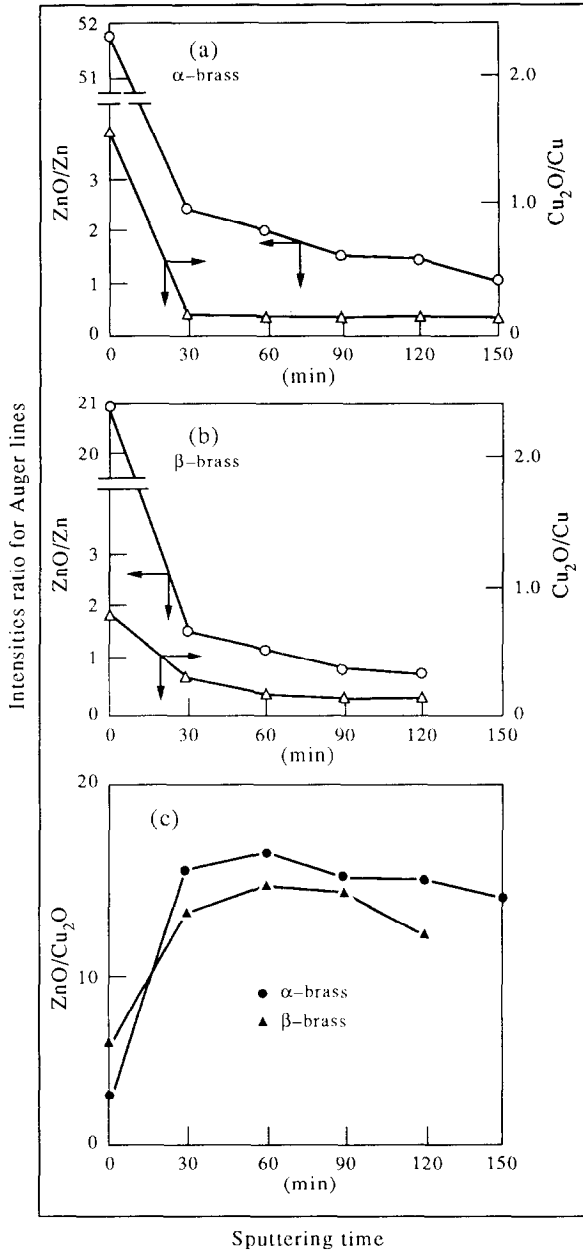


Fig. 4. Metal/oxide L<sub>3</sub>M<sub>45</sub>M<sub>45</sub> Auger line intensity ratio vs sputtering time plots. (a)  $\alpha$ -brass passivated at 0.0 V in borate-boric acid buffer + 0.5 M NaCl, ( $\Delta$ ) Cu<sub>2</sub>O/Cu, ( $\circ$ ) ZnO/Zn; (b)  $\beta$ -brass passivated at 0.0 V in borate-boric acid buffer + 0.5 M NaCl, ( $\Delta$ ) Cu<sub>2</sub>O/Cu, ( $\circ$ ) ZnO/Zn; and (c) ZnO/Cu<sub>2</sub>O L<sub>3</sub>M<sub>45</sub>M<sub>45</sub> Auger line intensity ratio vs sputtering time for ( $\bullet$ )  $\alpha$ -brass and ( $\blacktriangle$ )  $\beta$ -brass passivated at 0.0 V in borate-boric acid + 0.5 M NaCl.

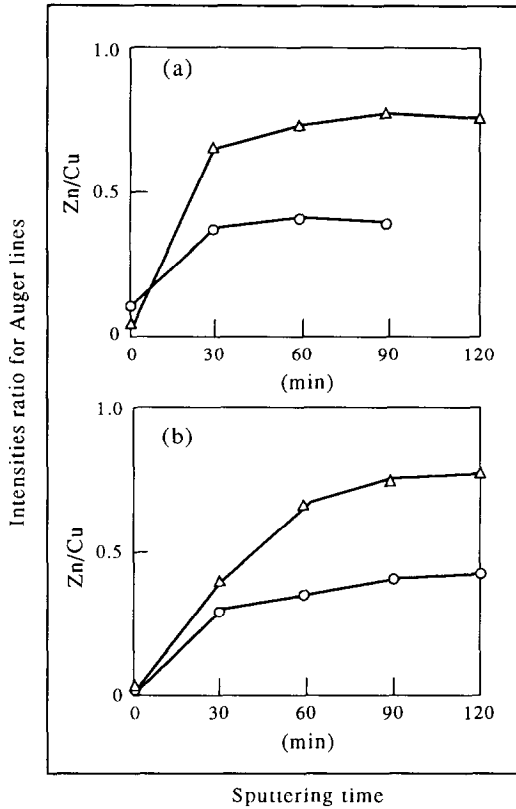


Fig. 5. Zn/Cu Auger  $L_3M_{45}M_{45}$  line intensity ratio vs sputtering time plots for  $\alpha$ -brass (O) and  $\beta$ -brass ( $\Delta$ ) electrodes anodized at 0.0 V in (a) borate-boric acid buffer; and (b) borate-boric acid buffer + 0.5 M NaCl.

alloy the initial  $Cu_2O/Cu$  ratio is greater and its evolution is opposed to that found in plain buffer. On the other hand, the initial  $ZnO/Zn$  intensity ratio is the same as that found in the absence of NaCl (Fig. 3b) and it reaches a nearly constant value for  $t_s > 60$  min. Hence, from these results, it can be concluded that for the passivated  $\beta$ -brass in NaCl-containing buffer the passive layer is thicker,  $h \cong 9$  nm, than in plain buffer, although it appears to be thinner as compared to the passive layer formed on passivated  $\alpha$ -brass in the NaCl-containing buffer.

For both,  $\alpha$ - and  $\beta$ -brass passivated in the borate-boric acid buffer + 0.5 M NaCl, the  $ZnO/Cu_2O$  ratio increases with  $t_s$  to reach a practically constant value for  $t_s > 30$  min (Fig. 4c). This indicates that the passive layer consists of an outer  $Cu_2O$ -rich and an inner ZnO rich layer. It should be noted that the relative amount of ZnO at the outer region of the passive layer is greater for the  $\beta$  alloy than for the  $\alpha$  alloy.

On the other hand, the Zn/Cu intensity ratio for  $\alpha$ - and  $\beta$ -brass after passivation at 0 V increases with  $t_s$  to attain nearly constant values for  $t_s > 30$  min in borate-boric acid (Fig. 5a), and for  $t_s > 60$  min in borate-boric acid + 0.5 M NaCl (Fig. 5b). These values approach those expected for the corresponding bulk alloys. The alloy surface consists of a Cu rich metal layer with  $l \cong 4-5$  nm in thickness in borate-boric acid and  $l \cong 10$  nm in thickness in 0.5 M NaCl + borate-boric acid buffer.

## DISCUSSION

The surface-sensitive XPS–AES techniques provide valuable information about the concentration of the various elements in the passive layers and in the atomic composition of first alloy layers. Results analysed in this work confirm the interpretation recently given<sup>1</sup> for the localized corrosion resistance of brass in both borate–boric acid and 0.5 M NaCl-containing borate–boric acid buffers. The AES data clearly show that in borate–boric acid a 4.5 nm thick complex passive layer consisting mainly of ZnO and Cu<sub>2</sub>O is formed irrespective of brass type. As observed for oxidized  $\alpha$ - and  $\beta$ -brass the main difference between these two alloys is the smaller relative amount of Cu<sub>2</sub>O constituent at the outer region in  $\beta$ -brass as compared to  $\alpha$ -brass.<sup>4</sup>

From earlier reported electrochemical data,<sup>1</sup> it was concluded that bulk CuO formation should occur only at potentials more positive than 0.25 V. This conclusion is also supported by AES data as only traces of CuO can be observed at the outer passive layer after brass passivation at 0 V. Unfortunately, Ar sputtering reduces CuO<sup>5</sup> so that no information can be found for this compound from depth profiles.

XPS and AES data also show that ZnO electroformation results in brass dezincification which implies the formation of a thin Cu-rich layer at the brass surface. This fact can be deduced from the evolution of the Zn/Cu intensity ratio.

The addition of NaCl to the buffer does not appreciably modify the composition of the passive layer, although the presence of NaCl makes some important changes in the passive layer characteristics. The outer region of the passive layer formed on both alloys becomes richer in Cu<sub>2</sub>O. This fact is related to the increase in depth of the dezincification region by the enhancement of Zn dissolution promoted by the Cl<sup>-</sup> ions.<sup>1</sup> This leads to the appearance of a thicker Cu rich layer on the alloy surface. This layer is covered by Cu<sub>2</sub>O after passivation at 0 V. The structure of the passive layer implies an outer Cu<sub>2</sub>O rich region. Furthermore, in NaCl-containing buffer, the passive layer for both  $\alpha$ - and  $\beta$ -brass, appears to be thicker than those formed on the plain buffer. However, for  $\beta$ -brass the passive layer becomes thinner than that formed on  $\alpha$ -brass. The relative high ZnO content at the outer region of the passive layer and the relatively small thickness of the passive layers can explain the lower resistance to the localized corrosion of the ( $\alpha + \beta$ )- and  $\beta$ -brass in relation to  $\alpha$ -brass.<sup>1</sup>

The presence of the thin Cu-rich surface layer accounts for the increase in localized corrosion resistance of brass with respect to Zn as the breakdown potential of the ZnO layer in the Cl<sup>-</sup>-ion-containing solution, as Cu-rich domains, which are immune to corrosion at potentials which are lower than that related to the Cu oxide formation, are exposed. The formation of a protective thin layer of the most noble metal constituent in the alloy hinders corrosion processes as it has been reported for other alloys at potentials more negative than the critical dealloying potential.<sup>6,7</sup> Results reported in this work allowed the conclusion that the thin layer of the most noble metal on the alloy surface also plays a relevant role in determining the localized corrosion resistance of brass.

## CONCLUSIONS

- (1) In the absence of NaCl, the passive layers formed at 0 V in  $\alpha$ - and  $\beta$ -brass are



predominantly made of ZnO and Cu<sub>2</sub>O. For the  $\alpha$ -brass the outer region of the passive film becomes richer in Cu<sub>2</sub>O, in contrast to  $\beta$ -brass. Only some traces of CuO can be detected at the outer region of the anodic layer formed at this potential.

(2) In 0.5 M NaCl-containing buffer the anodic layer composition found in the plain buffer remains unchanged, although the passive layer becomes comparatively thicker. For  $\beta$ -brass, the ZnO/Cu<sub>2</sub>O ratio at the outer region of the passive layer is greater and the thickness of the passive layer thinner than those found for  $\alpha$ -brass. These facts can explain the decrease in localized corrosion resistance of  $\beta$ -brass as compared to  $\alpha$ -brass and Cu.

(3) The overall Zn/Cu atomic ratio for the two alloys, change in depth in a rather similar way. The Cu-rich layer produced on the alloy surface by dezincification is deeper for those types of brass passivated in NaCl-containing buffer. The greater resistance of  $\alpha$ - and  $\beta$ -brass to localized corrosion in relation to Zn can be related to the presence of the Cu rich thin layer at the alloy surface produced during Zn electrodisolution and ZnO formation.

*Acknowledgements*—Authors thank UNELCO S. A. (Unión Eléctrica de Canarias S. A.) and Dirección General de Investigación Científica y Técnica (DGICYT) (Spain) for the financial support of this work. A.J.A. and R.C.S. thank CONICET (Argentina).

## REFERENCES

1. J. Morales, G. T. Fernández, P. Esparza, S. González, R. C. Salvarezza and A. J. Arvia, *Corros. Sci.* **37**, 211 (1995).
2. M. R. G. de Chialvo, R. C. Salvarezza, D. Vásquez Moll and A. J. Arvia, *Electrochim. Acta* **30**, 1501 (1985).
3. C. D. Wagner, W. M. Rigg, L. E. Davis, J. F. Moulder and G. E. Muilenberg, *Handbook of X-ray Photoelectrons Spectroscopy*, Perkin-Elmer Corporation, Minnesota (1979).
4. S. Maroic, R. Caudano and J. Verbist, *Surf. Sci.* **100**, 1 (1980).
5. D. F. Mitchell, G. I. Sproule and M. J. Graham, *Surf. Interfac. Anal.* **15**, 487 (1990).
6. H. W. Pickering, *Corros. Sci.* **23**, 1107 (1983).
7. T. P. Moffat, R. F. Fan and A. J. Bard, *J. electrochem. Soc.* **138**, 3224 (1991).